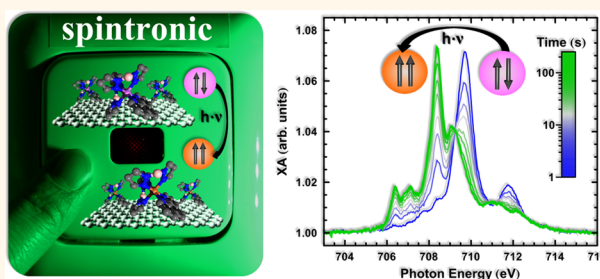


Highly Efficient Thermal and Light-Induced Spin-State Switching of an Fe(II) Complex in Direct Contact with a Solid Surface

Matthias Bernien,^{*,†} Holger Naggert,[‡] Lucas M. Arruda,[†] Lalminthang Kipgen,[†] Fabian Nickel,[†] Jorge Miguel,[†] Christian F. Hermanns,[†] Alex Krüger,[†] Dennis Krüger,[†] Enrico Schierle,[§] Eugen Weschke,[§] Felix Tuczek,[‡] and Wolfgang Kuch[†]

[†]Institut für Experimentalphysik, Freie Universität Berlin, Arnimallee 14, 14195 Berlin, Germany, [‡]Institut für Anorganische Chemie, Christian-Albrechts-Universität zu Kiel, Max-Eyth-Straße 2, 24098 Kiel, Germany, and [§]Helmholtz-Zentrum Berlin für Materialien und Energie, Albert-Einstein-Straße 15, 12489 Berlin, Germany

ABSTRACT Spin crossover (SCO) complexes possess a bistable spin state that reacts sensitively to changes in temperature or excitation with light. These effects have been well investigated in solids and solutions, while technological applications require the immobilization and contacting of the molecules at surfaces, which often results in the suppression of the SCO. We report on the thermal and light-induced SCO of [Fe(bpz)₂phen] molecules in direct contact with a highly oriented pyrolytic graphite surface. We are able to switch on the magnetic moment of the molecules by illumination with green light at $T = 6$ K, and off by increasing the temperature to 65 K. The light-induced switching process is highly efficient leading to a complete spin conversion from the low-spin to the high-spin state within a submonolayer of molecules. [Fe(bpz)₂phen] complexes immobilized on weakly interacting graphite substrates are thus promising candidates to realize the vision of an optically controlled molecular logic unit for spintronic devices.



KEYWORDS: spin crossover · molecular switches · light-induced excited spin-state trapping · surfaces · X-ray absorption spectroscopy

Using magnetic molecules as building blocks for spintronic devices is a promising approach for miniaturization of functional units since it provides structural control and reproducibility on the atomic level by the chemical design of the molecules.¹ Spin crossover (SCO) complexes are appealing because they possess a bistable spin state that reacts sensitively to external stimuli, such as changes in temperature or excitation with light. They can thus function as tiny molecular magnetic switches that can be controlled optically. SCO molecules consist of a transition-metal center surrounded by organic ligands that provide structural stability and prevent oxidation of the metal center. The bistability stems from a competition between the ligand field favoring an electronic occupation of the levels lowest in energy (low-spin (LS) state) and the spin-pairing energy

favoring a parallel alignment of the spins of the d electrons (high-spin (HS) state). Thermally induced SCO was first reported in 1931.² The SCO transition is entropy driven due to the different spin multiplicity and the different number of accessible vibrational levels of the LS and HS states giving rise to a temperature-dependent contribution to Gibbs free energy.³ In contrast, light-induced switching of the spin state is triggered by optical excitation of the metal-to-ligand charge-transfer (MLCT) band. The spin dynamics after the excitation has been recently observed using femtosecond X-ray pulses.⁴ After excitation the electronic state decays into the LS or HS state and can then be trapped if the energy barrier is high enough with respect to the thermal energy. Light-induced excited spin-state trapping (LIESST) was first observed in the early 80s of the last century.^{5,6}

* Address correspondence to bernien@physik.fu-berlin.de.

Received for review May 11, 2015 and accepted August 12, 2015.

Published online August 12, 2015
10.1021/acsnano.5b02840

© 2015 American Chemical Society

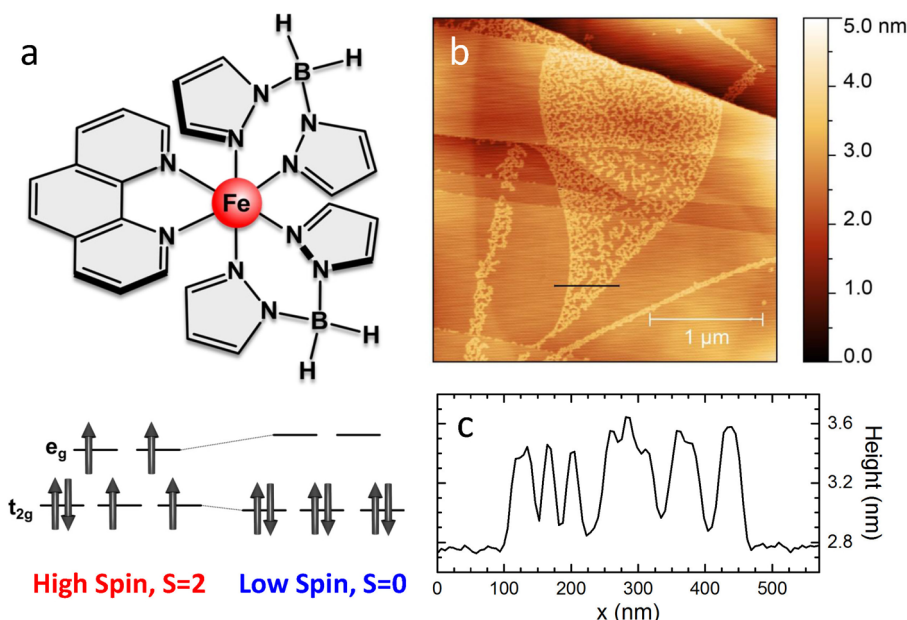


Figure 1. Sketch (a) of the molecular structure of $[\text{Fe}(\text{bpz})_2\text{phen}]$ and arrangement of the 3d electrons in the HS and LS state. AFM topography image (b) of 0.2 ML of $[\text{Fe}(\text{bpz})_2\text{phen}]$ on HOPG and line scan (c) across the molecular island along the black line in (b).

Since their discovery these phenomena have been intensively investigated.^{7–9} The studies were mostly carried out in solution, on powder samples, and on single crystals. Lately, a lot of research has been devoted to vacuum deposition of SCO molecules using neutral complexes.^{10–20} In this way addressability and immobilization are provided by the solid substrate. Recently, memristive behavior of a single SCO molecule on a CuN surface was reported using low-temperature scanning tunneling microscopy (STM).²¹ Only a few SCO complexes have been successfully evaporated onto surfaces. While decomposition of some fraction of molecules concomitant to the evaporation process was observed for $[\text{Fe}(\text{NCS})_2(\text{phen})_2]$ (phen = 1,10-phenanthroline)¹⁸ and $[\text{Fe}(\text{NCS})_2\text{L}]$ (L = 1-{6-[1,1-di(pyridin-2-yl)ethyl]-pyridin-2-yl}-N,N-dimethylmethanamine),¹⁷ $[\text{Fe}(\text{bpz})_2\text{phen}]$ (bpz = dihydrobis(pyrazolyl)borate), $[\text{Fe}(\text{bpz})_2\text{bipy}]$ (bipy = 2,2'-bipyridine), and $[\text{Fe}(\text{tpz})_2]$ (tpz = tris(pyrazolyl)borate) can be deposited very reliably due to their comparably low sublimation temperatures.^{10–12}

Partial thermal SCO and LIESST have been reported for $[\text{Fe}(\text{bpz})_2\text{bipy}]$ molecules on Au(111),²² but 80% of the molecules did not undergo a spin transition. It remains unclear what is the reason for the SCO of 20% of the molecules and whether they were in direct contact with the Au(111) surface. $[\text{Fe}(\text{bpz})_2\text{phen}]$ was found to decompose into $[\text{Fe}(\text{bpz})_2]$ and phen moieties when in direct contact with a Au(111) surface. Molecules in the second layer, on the other hand, stayed intact and showed thermal SCO.¹⁴ So far, four new analogues of the spin-crossover complex $[\text{Fe}(\text{bpz})_2\text{phen}]$ containing functionalized 1,10-phenanthroline ligands have been reported recently.²³

Here we report on the thermal SCO and LIESST of $[\text{Fe}(\text{bpz})_2\text{phen}]$ molecules in direct contact with a highly oriented pyrolytic graphite (HOPG) surface. In the submonolayer regime illumination with green light leads to a complete spin conversion from LS to HS at $T = 6$ K. The spin transition is fully reversible: when heated to 65 K all the molecules relax back to the LS state. Increasing the temperature to 300 K results in a thermally induced SCO of about 90% of the molecules.

RESULTS

Submonolayers of $[\text{Fe}(\text{bpz})_2\text{phen}]$ (Figure 1a) were prepared by sublimation in ultrahigh vacuum (UHV) onto an HOPG substrate held at room temperature. To ascertain that the molecules cover the surface and do not form three-dimensional crystallites, we have performed atomic force microscopy (AFM) measurements. In Figure 1b an AFM topography image of 0.2 ML of $[\text{Fe}(\text{bpz})_2\text{phen}]$ on HOPG is shown. The sample was prepared in UHV whereas the image subsequently was recorded under ambient conditions. In the submonolayer regime the molecules form porous islands with an average height of 0.7 nm (see Figure 1c), which matches the height of a single $[\text{Fe}(\text{bpz})_2\text{phen}]$ molecule. No formation of three-dimensional structures is observed. Although the AFM measurements were performed *ex-situ* and thus do not necessarily reflect the structure of molecular layers in a vacuum, we can conclude that the complexes are forming a molecular layer and that molecules of the first layer are in direct contact with the surface.

The spin state of the adsorbed molecules was monitored by means of X-ray absorption (XA) spectroscopy at the Fe $L_{2,3}$ edges providing submonolayer sensitivity

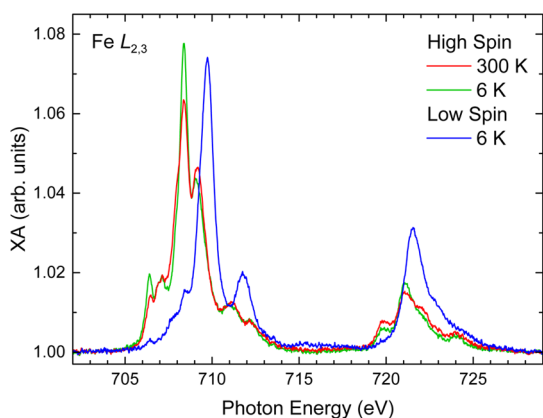


Figure 2. Temperature-dependent Fe $L_{2,3}$ XA spectra of 0.4 ML of $[\text{Fe}(\text{bpz})_2\text{phen}]$ on HOPG. Spectra before and after illuminating the sample with green light at $T = 6$ K are shown in blue and green, respectively.

and clearly distinguishable HS and LS spectra. The measurements were carried out with reduced X-ray photon flux to minimize the effect of soft X-ray-induced excited spin-state trapping (SOXIESST)^{24,25} below $T = 70$ K. Figure 2 shows the temperature- and light-induced spin-state switching of 0.4 ML of $[\text{Fe}(\text{bpz})_2\text{phen}]$ on HOPG. Fe $L_{2,3}$ XA spectra recorded at room temperature (red line) and $T = 6$ K (blue line) are distinctly different. In order to minimize the effect of SOXIESST, the latter spectrum was measured on a virgin position that had not been exposed to X-rays before. After illumination with green light for 34 min (Setup A, *cf.* Methods) at low temperature (green line), the Fe $L_{2,3}$ XA spectrum changes completely its shape and closely resembles the one recorded at 300 K. At room temperature and after illumination the Fe L_3 edge is composed of a double-peak structure with peaks at 708.4 and 709.1 eV. Before illumination at 6 K a single peak at 709.7 eV and a satellite peak at 711.8 eV are observed. The integrated intensity of the Fe L_3 edge with respect to the total integrated intensity, *i.e.*, the branching ratio, is 0.77(2) at room temperature, 0.67(2) at 6 K, and 0.79(2) after illumination at low temperature. The shift of the Fe $L_{2,3}$ resonance intensity toward higher photon energies, the change in line shape, and the reduction of the branching ratio are characteristic of a HS-to-LS transition and have been observed for similar SCO complexes.^{17,22,26} In a qualitative way the spectral changes between the HS and LS Fe L_3 XA spectra can be explained within a one-electron model in which XAS probes the unoccupied e_g and t_{2g} orbitals. In the HS state both e_g and t_{2g} levels have 2 holes giving rise to a double-peak feature in the spectrum. In the LS state only the e_g levels contain holes, resulting in a single peak. However, in a realistic picture the multi-electron nature of the initial and final state has to be taken into account, giving rise to a pronounced multiplet fine structure of the resonances as it is described within the atomic multiplet calculation presented in

the Supporting Information. The differences between the HS spectra at room temperature and at 6 K after illumination are attributed to the different thermal population of HS states closely spaced in energy and are reproduced by the calculations.

In contrast to SCO complexes adsorbed on Au(111),^{14,15,22} the spin transition appears to be virtually complete at submonolayer coverage. Thus, the SCO transition is not hindered by the direct contact of the molecules with the HOPG substrate. This different behavior can be attributed to a weaker molecule–substrate interaction on HOPG compared to Au(111), preserving the integrity of the molecule.

When cooling the sample from room temperature down to $T = 6$ K, the Fe L_3 XA spectra change gradually from the HS to the LS spectra (see Supporting Information). To determine the HS fraction, the spectra shown in Figure 2 were used as a reference and each spectrum was fitted as a linear combination. In the temperature range between 300 and 65 K the HS spectrum at 300 K and the LS spectrum at 6 K and in the temperature range below 65 K the HS spectrum at 6 K and the LS spectrum at 6 K were used as a reference. The HS spectrum after illumination at $T = 6$ K was defined as 100% HS, since the time constant of the metastable HS state was determined to be 21 h (see below) and the cross-section for exciting a HS-to-LS transition (reverse LIESST) is typically 3 orders of magnitude lower than LIESST exciting the metal-to-ligand charge-transfer band. The LS spectrum shown in Figure 2 was measured on a virgin position and thus contains minimum SOXIESST. This was defined as 100% LS. The HS fraction of the spectrum at 300 K (91%) is obtained from the fit of a thermo-dynamical model without cooperative effects as described below. By comparison to the calculated spectra of pure HS and LS configuration (see Supporting Information), the resulting systematic errors are estimated to be smaller than 5%. The fraction of HS molecules as a function of temperature is plotted in Figure 3. Between 300 and 70 K it gradually decreases, as is expected for a thermal spin transition. Below 70 K the HS fraction increases with decreasing temperature, which can be attributed to SOXIESST.^{24,25}

The temperature at which half of the molecules are in the HS state is $T_{1/2} = 162(4)$ K, which is the same within error as for the bulk system.²⁷ The width of the transition defined as the difference between the temperatures at which 80% of the molecules are in the HS and LS states, respectively, is $\Delta T_{80} = 83(6)$ K. This is lower than for a submonolayer of $[\text{Fe}(\text{NCS})_2\text{L}]$ on HOPG,¹⁷ suggesting a higher uniformity in the intermolecular and molecule–substrate interactions. With respect to $[\text{Fe}(\text{bpz})_2\text{phen}]$ bulk material^{14,27,28} the width of the transition is strongly increased due to the lack of cooperativity between the molecules in the submonolayer during the transition. Indeed, the thermal

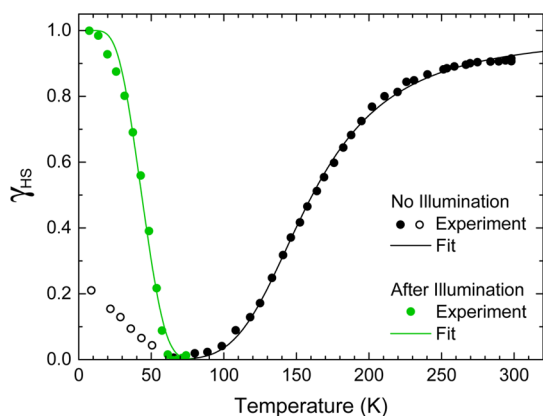


Figure 3. Fraction of HS molecules as a function of temperature during cooling the sample without illumination (black solid symbols) and after saturation of the light-induced HS state during heating the sample (green solid symbols). The temperature-induced SCO is fitted with a model without cooperative interactions between the molecules (black line). The relaxation of the light-induced HS state is fitted with an Arrhenius law (green line). Below 70 K (black open symbols), the molecules undergo an X-ray induced transition to the HS state caused by the measurement.

spin transition can be described by a model without cooperative interactions between the molecules. The transition is driven by the difference in entropy ΔS between the HS and LS states, which is a consequence of the higher number of accessible vibrational states and the higher spin multiplicity of the HS state. With ΔH and R being the enthalpy difference between the HS and LS states and the gas constant, respectively, the fraction of HS molecules is calculated from the thermodynamic equilibrium condition as³

$$\gamma_{\text{HS}}(T) = (e^{\Delta H/(RT)} - \Delta S/R + 1)^{-1} \quad (1)$$

Fitting this model to the experimental data shown in Figure 3 (black solid symbols) yields $\Delta S = 45(3) \text{ J K}^{-1} \text{ mol}^{-1}$ and $\Delta H = 7.2(5) \text{ kJ mol}^{-1}$, which are slightly lower than in the bulk material.²⁷ Since both the interaction between molecules as well as between molecules and the surface is expected to be low, the molecules are likely to be mobile at submonolayer coverage, dynamically forming islands and two-dimensional gas-like phases at ambient temperatures. Identical spectra are obtained after cycling between HS and LS states, which indicates that always the same macroscopic state is reached.

After illumination with green light for 39 min (Setup A, *cf.* Methods) at 6 K the molecules are in the HS state due to LIESST. At $T = 6 \text{ K}$ the relaxation to the LS state is very slow: waiting for 12.3 h without illumination resulted in a HS fraction of 0.56 corresponding to a time constant of 21 h. This value is significantly lower than for the bulk material where a HS fraction of 0.96 was observed after waiting for 12 h at $T = 10 \text{ K}$.²⁷ The difference may be ascribed to the higher degree of freedom of the complexes in the molecular layer or to a

structural distortion of the molecules due to the interaction with the surface. A destabilization of the HS state at low temperatures was also observed for ultrathin films of $[\text{Fe}(\text{bpz})_2\text{phen}]$ on Au(111).²⁰

We have measured the relaxation to the LS state while heating the sample from 6 to 74 K with a heating rate of 4 K/min after illumination. The Fe L_3 XA spectra change gradually from the HS to LS spectrum (see Supporting Information). The fraction of HS molecules is determined by fitting a linear combination of the HS spectrum at 6 K and the LS spectrum at 6 K, shown in Figure 2. The fraction of HS molecules as a function of temperature, shown in Figure 3 (green symbols), decreases rapidly with temperature, so that at 65 K all molecules are in the LS state. Fitting the relaxation data to an Arrhenius law according to

$$\gamma_{\text{HS}}(t) = e^{-A \int_0^t e^{-E_a/(RT(t))} dt} \quad (2)$$

with $T(t)$ being the temperature as a function of time, leads to an effective energy barrier $E_a = 789(90) \text{ J mol}^{-1}$ and a pre-exponential factor $A = 0.032(9) \text{ s}^{-1}$. The effective barrier height is about a factor of 2.6 lower than in the bulk material,²⁷ again indicating that the HS state is destabilized on the HOPG surface. Note that the fit using eq 2 is purely phenomenological, since the underlying mechanism of the HS-to-LS relaxation with increasing temperature is quantum tunneling *via* thermally activated vibrational levels.³ The value of the prefactor as determined by the fit is close to 0.05 s^{-1} found for bulk material.²⁷

We have studied the photochromic response of 0.4 ML of $[\text{Fe}(\text{bpz})_2\text{phen}]$ on HOPG by recording the Fe L_3 XA spectrum at $T = 6 \text{ K}$ as a function of exposure to green light of 520 nm wavelength and a flux density of $\phi = 4.2(8) \times 10^{14} \text{ photons s}^{-1} \text{ mm}^{-2}$ (Setup A, *cf.* Methods). This wavelength was chosen based on UV-vis spectroscopy measurements of a thin film of $[\text{Fe}(\text{bpz})_2\text{phen}]$ on glass presented in ref 10. In the LS state, the complex shows a broad absorption band from 480 to 640 nm. Again, the HS fraction of the individual spectra is determined by fitting linear combinations of the pure HS (6 K) and LS (6 K) spectra (Figure 2) and is shown in Figure 4. The spin conversion is highly efficient with a time constant of $\tau = 20.4(7) \text{ s}$. This corresponds to an effective cross section of $\sigma_{\text{eff}} = (\phi\tau)^{-1} = 0.012(3) \text{ \AA}^2$. Comparing to the value $\sigma = 0.137 \text{ \AA}^2$ found for bulk,^{10,20} one has to consider the decrease in intensity of the green light in the proximity of the surface. For HOPG the superposition of incoming and reflected light results in a reduction in intensity by about a factor of 4 at the position of the molecule.²⁹ The spin-state switching is fully reversible: after heating the sample to 65 K the molecules switch back to the LS state (see Figure 3).

To monitor the magnetic properties we have performed X-ray magnetic circular dichroism (XMCD)

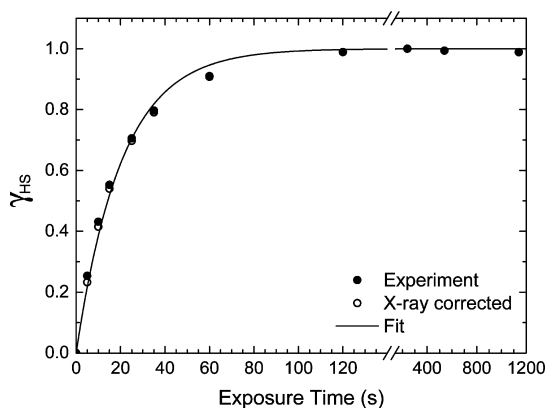


Figure 4. Fraction of HS molecules as a function of exposure to green light at $T = 6$ K and fit of an exponential model to the data after correction for SOXIESST.

measurements in an external magnetic field of 5.9 T at a temperature of 6 K. The XMCD signal, *i.e.*, the difference in absorption of left- and right-circularly polarized X-rays, is directly proportional to the magnetization of the molecules. The Fe $L_{2,3}$ XA and XMCD spectra of 0.4 ML of $[\text{Fe}(\text{bpz})_2\text{phen}]$ on HOPG are shown in Figure 5. Before illumination (blue lines), the Fe $L_{2,3}$ XA spectrum (top panel) corresponds to the LS, $S = 0$, state, which would yield a null XMCD signal. The measured dichroism, however, presents a tiny amplitude, as small as 5% of the XA signal. This is a consequence of SOXIESST during the measurement, which can not be fully suppressed at low temperatures. After illumination with green light of 520 nm wavelength (Setup B, *cf.* Methods) for 46 min (red lines), a clear XMCD signal is visible similar to the one observed for a thin film of $[\text{Fe}(\text{bpz})_2\text{bipy}]$ on Au(111).²² Due to a much lower flux density compared to the data shown in Figure 4, the HS fraction after illumination, determined by fitting the XA spectrum with the XA data of the HS (6 K) and LS (6 K) states shown in Figure 2, is 0.75. However, the XMCD signal only stems from HS molecules and thus reflects their magnetic properties. The XMCD measurements demonstrate the magnetic nature of the difference between the two electronic states

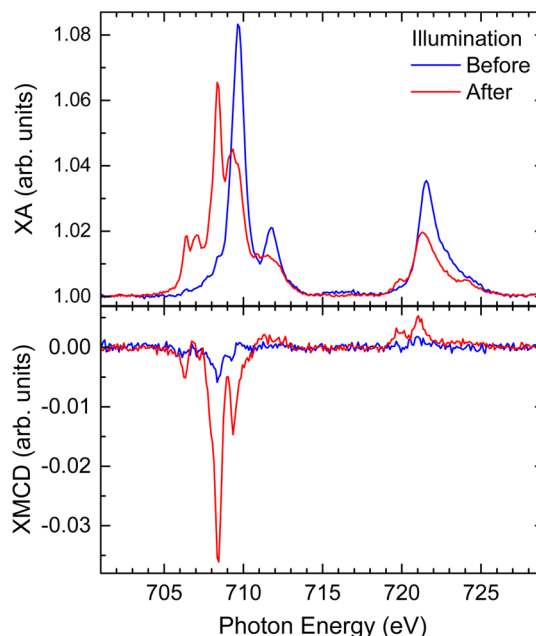


Figure 5. Fe $L_{2,3}$ XA and XMCD spectra of 0.4 ML $[\text{Fe}(\text{bpz})_2\text{phen}]$ on HOPG before illumination and after illumination with green light. The spectra are measured in an applied magnetic field of 5.9 T at a temperature of 6 K.

and prove that the Fe magnetic moment is switched by green light.

CONCLUSIONS

We have shown that the magnetic moment of $[\text{Fe}(\text{bpz})_2\text{phen}]$ molecules that are in direct contact with an HOPG surface can be switched on by illumination with green light at $T = 6$ K, and off by increasing the temperature to 65 K. The light-induced switching process is highly efficient with a time constant of 20.4(7) s at a flux density of $4.2(8) \times 10^{14}$ photons $\text{s}^{-1} \text{mm}^{-2}$ leading to a complete spin conversion from the LS to the HS state within a submonolayer of molecules. $[\text{Fe}(\text{bpz})_2\text{phen}]$ complexes thus preserve their spin switching capabilities even when immobilized on a graphite substrate. This is of considerable interest with respect to optical control in molecular spin electronics.

METHODS

All XA experiments were performed at the high-field diffractometer of the beamline UE46-PGM1 at BESSY II providing linearly and circularly polarized X-rays with 99% and 85% degree of polarization, respectively, at the third harmonic of the undulator. The energy resolution was set to approximately 150 meV. The photon flux was reduced by a factor of 15 by means of a 3 μm thick Al foil inserted into the beam to minimize X-ray-induced spin-state switching of the molecules below $T = 70$ K. The photon flux density at the position of the sample was then about 10^9 photons $\text{s}^{-1} \text{mm}^{-2}$ with a spot size of about 1 mm^2 . Besides the reversible LS to HS conversion due to the SOXIESST effect, no irreversible time-dependent modifications of the XA spectra were observed. We can thus exclude radiation-damage effects for the presented measurements. The XA signal was recorded in total electron yield (TEY) mode measuring the

drain current of the sample as a function of photon energy. This signal was normalized to the TEY of a gold grid upstream to the experiment. For the measurements presented in Figure 5 the signal of the refocusing mirror was used for normalization. The resulting spectra were normalized to the spectra of a clean HOPG substrate without adsorbed molecules. XA spectra were recorded at the magic angle of incidence, that is, 54.7° and 35.3° between the k vector of the X-rays and the surface when using linearly p -polarized and circularly polarized X-rays, respectively. At this angle the XA resonance intensities are independent of the orientations of the molecular orbitals.

$[\text{Fe}(\text{bpz})_2\text{phen}]$ was synthesized according to the literature.²⁸ High quality (ZYA) 12 mm \times 12 mm \times 2 mm HOPG substrates exhibiting a mosaic spread angle of 0.4(1)° were purchased from Structure Probe. A clean HOPG surface was prepared by cleaving an HOPG substrate at a pressure of

10^{-6} mbar by means of a carbon tape. $[\text{Fe}(\text{bpz})_2\text{phen}]$ was evaporated in UHV at a pressure of about 2×10^{-9} mbar from a tantalum Knudsen cell at about 435 K and deposited onto the substrate held at room temperature. All XAS and XMCD measurements were carried out at a pressure of about 5×10^{-11} mbar. Coverages were estimated by using a quartz microbalance and the integrated $\text{Fe } L_3$ resonance intensity. Following the procedure described in ref 14, the Fe XA signal was compared to that of an Fe octaethyl-porphyrin (Cl)/Cu(001) reference sample, which had been measured both with STM and XAS.³⁰ An areal density of $0.82 \text{ Fe ions/nm}^2$ was assumed for one ML. The XA intensity ratio between HOPG and Cu(001) substrates in the pre-edge region of the Fe L_3 edge has been determined by XA measurements under identical conditions with normalization to the gold grid. Clean HOPG and Cu(001) substrates show X-ray absorption intensities different by a factor of 0.78(8) at 700 eV photon energy. With increasing coverage the background signal of Cu(001) increases, due to the decrease in work function, whereas the background signal of HOPG remains unchanged. For a coverage of one monolayer the intensity ratio between these two substrates is 0.61(7).

AFM was performed on a Nanotec Cervantes instrument using the tapping mode of a Si cantilever with a stiffness of 2.7 N/m at a resonance frequency of 75 kHz. These measurements have been carried out in ambient conditions after preparation of the sample in vacuum by the same procedure as for the XA experiments. Illumination was carried out by means of a green LED with a wavelength of $\lambda = 520 \text{ nm}$ and a full width at half-maximum (fwhm) of 30 nm (Setup A). The radiated optical power was about 400 mW. The light was collimated by an aspherical and a spherical lens with a focal length of 32 and 500 mm, respectively. The light entered the UHV chamber through a window in a distance of 575 mm from the sample. The flux density at the sample position was $\phi = 4.2(8) \times 10^{14} \text{ photons s}^{-1} \text{ mm}^{-2}$. For the measurements presented in Figure 5 a different optical setup was used (Setup B). The white light of a 1000 W arc lamp was filtered by an infrared water filter, a cold-light mirror and an interference filter with a wavelength of 520 nm and a fwhm of 10 nm. The flux density was about 2 orders of magnitude lower than the one of Setup A.

Conflict of Interest: The authors declare no competing financial interest.

Acknowledgment. A. Britton, V. Mazalova, W. Walter, and N. Blümel are acknowledged for their support during the beam-times. C. Lotze is acknowledged for his help with the AFM measurements. Financial support by the DFG through Sfb 677 and 658 is gratefully acknowledged.

Supporting Information Available: The Supporting Information is available free of charge on the ACS Publications website at DOI: 10.1021/acsnano.5b02840.

Higher coverage AFM topography, temperature- and exposure-dependent Fe L_3 XA spectra, charge-transfer multiplet calculations. (PDF)

REFERENCES AND NOTES

1. Auwärter, W.; Ćija, D.; Klappenberger, F.; Barth, J. V. Porphyrins at Interfaces. *Nat. Chem.* **2015**, *7*, 105–120.
2. Cambi, L.; Szegő, L. Über die magnetische Suszeptibilität der komplexen Verbindungen. *Ber. Dtsch. Chem. Ges. B* **1931**, *64*, 2591–2598.
3. Hauser, A.; Jeftić, J.; Romstedt, H.; Hinek, R.; Spiering, H. Cooperative Phenomena and Light-Induced Bistability in Iron(II) Spin-Crossover Compounds. *Coord. Chem. Rev.* **1999**, *190*, 471–491.
4. Zhang, W.; Alonso-Mori, R.; Bergmann, U.; Bressler, C.; Chollet, M.; Galler, A.; Gawelda, W.; Hadt, R. G.; Hartsock, R. W.; Kroll, T.; *et al.* Tracking Excited-State Charge and Spin Dynamics in Iron Coordination Complexes. *Nature* **2014**, *509*, 345–348.
5. McGarvey, J. J.; Lawthers, I. Photochemically-Induced Perturbation of the $^1A \rightleftharpoons ^5T$ Equilibrium in Fe^{II} Complexes by Pulsed Laser Irradiation in the Metal-to-Ligand Charge-Transfer Absorption Band. *J. Chem. Soc., Chem. Commun.* **1982**, 906–907.
6. Decurtins, S.; Güttlich, P.; Köhler, C. P.; Spiering, H.; Hauser, A. Light-Induced Excited Spin State Trapping in a Transition-Metal Complex: The Hexa-1-Propyltetrazole-Iron (II) Tetrafluoroborate Spin-Crossover System. *Chem. Phys. Lett.* **1984**, *105*, 1–4.
7. Güttlich, P.; Gaspar, A. B.; Garcia, Y. Spin State Switching in Iron Coordination Compounds. *Beilstein J. Org. Chem.* **2013**, *9*, 342–391.
8. Halcrow, M. A., Ed.; *Spin-Crossover Materials: Properties and Applications*; John Wiley & Sons, Ltd.: New York, 2013.
9. Special Issue: Spin-Crossover Complexes. *Eur. J. Inorg. Chem.* **2013**, 574–1067.
10. Naggert, H.; Bannwarth, A.; Chemnitz, S.; von Hofe, T.; Quandt, E.; Tuczek, F. First Observation of Light-Induced Spin Change in Vacuum Deposited Thin Films of Iron Spin Crossover Complexes. *Dalton Trans.* **2011**, *40*, 6364–6366.
11. Palamarciuc, T.; Oberg, J. C.; El Hallak, F.; Hirjibehedin, C. F.; Serri, M.; Heutz, S.; Létard, J.-F.; Rosa, P. Spin Crossover Materials Evaporated under Clean High Vacuum and Ultra-High Vacuum Conditions: from Thin Films to Single Molecules. *J. Mater. Chem.* **2012**, *22*, 9690–9695.
12. Mahfoud, T.; Molnár, G.; Cobo, S.; Salmon, L.; Thibault, C.; Vieu, C.; Demont, P.; Bousseksou, A. Electrical Properties and Non-Volatile Memory Effect of the $[\text{Fe}(\text{HB}(\text{pz})_3)_2]$ Spin Crossover Complex Integrated in a Microelectrode Device. *Appl. Phys. Lett.* **2011**, *99*, 053307.
13. Gopakumar, T. G.; Matino, F.; Naggert, H.; Bannwarth, A.; Tuczek, F.; Berndt, R. Electron-Induced Spin Crossover of Single Molecules in a Bilayer on Gold. *Angew. Chem., Int. Ed.* **2012**, *51*, 6262–6266.
14. Gopakumar, T. G.; Bernien, M.; Naggert, H.; Matino, F.; Hermanns, C. F.; Bannwarth, A.; Mühlenerend, S.; Krüger, A.; Krüger, D.; Nickel, F.; *et al.* Spin-Crossover Complex on Au(111): Structural and Electronic Differences Between Mono- and Multilayers. *Chem. - Eur. J.* **2013**, *19*, 15702–15709.
15. Pronschinske, A.; Chen, Y.; Lewis, G. F.; Shultz, D. A.; Calzolari, A.; Buongiorno Nardelli, M.; Dougherty, D. B. Modification of Molecular Spin Crossover in Ultrathin Films. *Nano Lett.* **2013**, *13*, 1429–1434.
16. Pronschinske, A.; Bruce, R. C.; Lewis, G.; Chen, Y.; Calzolari, A.; Buongiorno-Nardelli, M.; Shultz, D. A.; You, W.; Dougherty, D. B. Iron(II) Spin Crossover Films on Au(111): Scanning Probe Microscopy and Photoelectron Spectroscopy. *Chem. Commun.* **2013**, *49*, 10446–10452.
17. Bernien, M.; Wiedemann, D.; Hermanns, C. F.; Krüger, A.; Rolf, D.; Kroener, W.; Müller, P.; Grohmann, A.; Kuch, W. Spin Crossover in a Vacuum-Deposited Submonolayer of a Molecular Iron(II) Complex. *J. Phys. Chem. Lett.* **2012**, *3*, 3431–3434.
18. Ellingsworth, E. C.; Turner, B.; Szulczewski, G. Thermal Conversion of $[\text{Fe}(\text{phen})_3](\text{SCN})_2$ Thin Films into the Spin Crossover Complex $\text{Fe}(\text{phen})_2(\text{NCS})_2$. *RSC Adv.* **2013**, *3*, 3745–3754.
19. Schäfer, B.; Rajnák, C.; Šalitroš, I.; Fuhr, O.; Klar, D.; Schmitz-Antoniak, C.; Weschke, E.; Wende, H.; Ruben, M. Room Temperature Switching of a Neutral Molecular Iron(II) Complex. *Chem. Commun.* **2013**, *49*, 10986–10988.
20. Ludwig, E.; Naggert, H.; Källäne, M.; Rohlf, S.; Kröger, E.; Bannwarth, A.; Quer, A.; Rosnagel, K.; Kipp, L.; Tuczek, F. Iron(II) Spin-Crossover Complexes in Ultrathin Films: Electronic Structure and Spin-State Switching by Visible and Vacuum-UV Light. *Angew. Chem., Int. Ed.* **2014**, *53*, 3019–3023.
21. Miyamachi, T.; Gruber, M.; Davesne, V.; Bowen, M.; Boukari, S.; Joly, L.; Scheurer, F.; Rogez, G.; Yamada, T. K.; Ohresser, P.; *et al.* Robust Spin Crossover and Memristance across a Single Molecule. *Nat. Commun.* **2012**, *3*, 938.
22. Warner, B.; Oberg, J. C.; Gill, T. G.; el Hallak, F.; Hirjibehedin, C. F.; Serri, M.; Heutz, S.; Arrio, M.-A.; Sainctavit, P.; Mannini, M.; *et al.* Temperature- and Light-Induced Spin Crossover Observed by X-Ray Spectroscopy on Isolated Fe(II) Complexes on Gold. *J. Phys. Chem. Lett.* **2013**, *4*, 1546–1552.
23. Naggert, H.; Rudnik, J.; Kippen, L.; Bernien, M.; Nickel, F.; Arruda, L. M.; Kuch, W.; Näther, C.; Tuczek, F. Vacuum-Evaporable Spin-Crossover Complexes: Physicochemical

- Properties in the Crystalline Bulk and in Thin Films Deposited from the Gas Phase. *J. Mater. Chem. C* **2015**, *3*, 7870–7877.
24. Davesne, V.; Gruber, M.; Miyamachi, T.; Da Costa, V.; Boukari, S.; Scheurer, F.; Joly, L.; Ohresser, P.; Otero, E.; Choueikani, F.; *et al.* First Glimpse of the Soft X-Ray Induced Excited Spin-State Trapping Effect Dynamics on Spin Cross-Over Molecules. *J. Chem. Phys.* **2013**, *139*, 074708.
 25. Collison, D.; Garner, C. D.; McGrath, C. M.; Mosselmans, J. F. W.; Roper, M. D.; Seddon, J. M. W.; Sinn, E.; Young, N. A. Soft X-Ray Induced Excited Spin State Trapping and Soft X-Ray Photochemistry at the Iron L_{2,3} Edge in [Fe(phen)₂(NCS)₂] and [Fe(phen)₂(NCSe)₂] (phen = 1,10-phenanthroline). *J. Chem. Soc., Dalton Trans.* **1997**, 4371–4376.
 26. Cartier dit Moulin, C.; Rudolf, P.; Flank, A. M.; Chen, C. T. Spin Transition Evidenced by Soft X-ray Absorption Spectroscopy. *J. Phys. Chem.* **1992**, *96*, 6196–6198.
 27. Moliner, N.; Salmon, L.; Capes, L.; Muñoz, M. C.; Létard, J.-F.; Bousseksou, A.; Tuchagues, J.-P.; McGarvey, J. J.; Dennis, A. C.; Castro, M.; *et al.* Thermal and Optical Switching of Molecular Spin States in the {[FeL(H₂B(pz)₂)₂] Spin-Crossover System (L = bpy, phen)}. *J. Phys. Chem. B* **2002**, *106*, 4276–4283.
 28. Real, J. A.; Muñoz, M. C.; Faus, J.; Solans, X. Spin Crossover in Novel Dihydrobis(1-pyrazolyl)borate [H₂B(pz)₂]-Containing Iron(II) Complexes. Synthesis, X-ray Structure, and Magnetic Properties of [FeL{H₂B(pz)₂}₂] (L = 1,10-Phenanthroline and 2,2'-Bipyridine). *Inorg. Chem.* **1997**, *36*, 3008–3013.
 29. Jellison, G. E.; Hunn, J. D.; Lee, H. N. Measurement of Optical Functions of Highly Oriented Pyrolytic Graphite in the Visible. *Phys. Rev. B: Condens. Matter Mater. Phys.* **2007**, *76*, 085125.
 30. Herper, H. C.; Bernien, M.; Bhandary, S.; Hermanns, C. F.; Krüger, A.; Miguel, J.; Weis, C.; Schmitz-Antoniak, C.; Krumme, B.; Bovenschen, D.; *et al.* Iron Porphyrin Molecules on Cu(001): Influence of Adlayers and Ligands on the Magnetic Properties. *Phys. Rev. B: Condens. Matter Mater. Phys.* **2013**, *87*, 174425.